

The VIMOS VLT Deep Survey: ★

Tracing the galaxy stellar mass assembly history over the last 8 Gyr

D. Vergani¹, M. Scodreggio¹, L. Pozzetti², A. Iovino³, P. Franzetti¹, B. Garilli¹, G. Zamorani², D. Maccagni¹, F. Lamareille², O. Le Fèvre⁴, S. Charlot^{5,6}, T. Contini⁷, D. Bottini¹, V. Le Brun⁴, J.P. Picat⁷, R. Scaramella^{8,9}, L. Tresse⁴, G. Vettolani⁸, A. Zanichelli⁸, C. Adami⁴, S. Arnouts⁴, S. Bardelli², M. Bolzonella², A. Cappi², P. Ciliegi², S. Foucaud¹⁰, I. Gavignaud¹¹, L. Guzzo³, O. Ilbert¹², H.J. McCracken^{6,13}, B. Marano¹⁴, C. Marinoni¹⁵, A. Mazure⁴, B. Meneux^{1,2}, R. Merighi², S. Paltani^{16,17}, R. Pellò⁷, A. Pollo^{4,18}, M. Radovich¹⁹, E. Zucca², M. Bondi⁸, A. Bongiorno¹⁴, J. Brinchmann²⁰, O. Cucciati^{3,21}, S. de la Torre⁴, L. Gregorini⁸, Y. Mellier^{6,13}, P. Merluzzi¹⁹, S. Tempurin³, and C.J. Walcher⁴

(Affiliations can be found after the references)

Received —; accepted —

ABSTRACT

Aims. Investigating the history of mass assembly for galaxies of different stellar masses and types.

Methods. We select a mass limited sample of 4048 objects from the VIMOS VLT Deep Survey (VVDS) in the redshift interval $0.5 \leq z \leq 1.3$. We then use an empirical criterion, based on the amplitude of 4000Å Balmer break (D_n4000) to separate the galaxy population in spectroscopically early- and late-type systems. The equivalent width of the [OII]3727 line is used as proxy for the star formation activity. We also derive type-dependent stellar mass function in three redshift bins.

Results. We discuss to which extent stellar mass drives galaxy evolution, showing for the first time a direct comparison of stellar ages and stellar masses over the last 8 Gyr. Low-mass galaxies have small D_n4000 and at increasing stellar mass the galaxy distribution moves to higher D_n4000 values as observed in the local Universe (Kauffmann et al. 2004). We witness an increasing abundance of massive spectroscopically early-type systems at the expenses of the late-type systems with cosmic time. This spectral transformation of late-type systems into old massive galaxies at lower redshift, confirmed by the evolution of our type-dependent stellar mass function, is a process started at early epochs ($z > 1.3$) that continues efficiently down to the local Universe. The underlying stellar ages of late-type galaxies apparently do not show evolution, most likely as a result of a continuous and efficient formation of new stars. All star formation activity indicators consistently point towards a star formation history peaked in the past for massive galaxies, with little or no residual star formation taking place at all observed epochs. Vice-versa most of the low-mass systems show just the opposite characteristics with significant star formation still presents at all epochs. The activity and efficiency of forming stars are mechanisms depending on galaxy stellar mass, resulting in a largely inefficient stellar mass assembly in massive systems up to $z = 1.3$. The concepts of downsizing in star formation and in mass (or archaeological downsizing) describe a single scenario which has a top-down evolutionary pattern in star formation as well as in mass assembly. The role of (dry) merging events seems to be only marginal at $z < 1.3$, as our estimated efficiency in stellar mass assembly can account for the progressive accumulation of observed passively evolving galaxies.

Key words. Galaxies: formation - galaxies: evolution - galaxies: fundamental parameters - galaxies: mass function - cosmology: observations

1. Introduction

How galaxies form and evolve with cosmic time is one of the key questions in observational cosmology. A fundamental role in this context is played by deep surveys sampling over thousand galaxies on large portions of the sky. The global star formation history is reasonably well known out to very high redshifts and with considerable details up to $z \sim 1$ (see for a recent summary Hopkins & Beacom 2006), but the role of the various physical mechanisms contributing to the assembly of galaxy stellar mass is still unclear, along with their importance at different epochs.

In agreement with the first formulation introduced by Cowie et al. (1996), a downsizing scenario for galaxy for-

mation emerges insistently in several observational studies (Brinchmann & Ellis 2000; Gavazzi et al. 2002; Kodama et al. 2004; Bauer et al. 2005; Feulner et al. 2005a,b; Juneau et al. 2005; Bundy et al. 2006; Borch et al. 2006; Cimatti et al. 2006, Pozzetti et al. 2007). However, observed galactic-scale properties like the quenching of star formation activity in massive galaxies are not yet ultimately reproduced within the Λ CDM framework (e.g. De Lucia et al. 2006; Bower et al. 2006) that successfully describes the hierarchical growth of dark matter halos and the galaxy clustering properties.

The observed discrepancies between models and observations are probably due to our limited ability to reproduce the actual physics on galactic scales with simple recipes. Possibly some feedback mechanisms are still missing in models. Thus, a phenomenological approach to the problem of the stellar mass assembly as a function of cosmic time, i.e. relying as much as possible on observational data, can suggest new implementations to current semi-analytical models.

Send offprint requests to: D. Vergani, e-mail: daniela@lambrate.inaf.it

* Based on data obtained with the European Southern Observatory Very Large Telescope, Paranal, Chile, program 070.A-9007(A), and on data obtained at the Canada-France-Hawaii Telescope, operated by the CNRS in France, CNRC in Canada and the University of Hawaii.

In this paper we use the first epoch observations of the VIMOS-VLT Deep Survey (VVDS, Le Fèvre et al. 2005) to derive stellar masses, stellar ages and star formation efficiency for a statistically significant sample of galaxies. VVDS is the first large spectroscopic survey for which an analysis on the efficiency in stellar mass assembly can be pursued starting from a time when the Universe had $\sim 30\%$ of its present age, covering up to the end of the most active phase of star formation.

The present work is organized as follows: the data and sample selection are presented in Section 2; the methodology we adopted to perform our analysis is described in Section 3. Results are given in Sect. 4 and a Summary in Sections 5. Throughout this work we assume a standard cosmological model with $\Omega_M = 0.3$, $\Omega_\Lambda = 0.7$ and $H_0 = 70 \text{ km s}^{-1} \text{ Mpc}^{-1}$. Magnitudes are given in the AB system.

2. The first epoch VVDS sample

The primary observational goal of the VVDS as well as the survey strategies are presented in Le Fèvre et al. (2005). Here is enough to stress that in order to minimize possible selection biases, the VVDS has been conceived as a purely flux-limited survey, i.e. no target pre-selection according to colors or compactness is implemented. In this paper we consider the deep spectroscopic sample of the first epoch data in the VVDS-0226-04 field (from now on simply VVDS-F02), that targets objects in the magnitude range $17.5 \leq I_{AB} \leq 24$.

First-epoch spectroscopic observations in the VVDS-F02 field were carried out with the VIMOS multi-object spectrograph (Le Fèvre et al. 2005). The $1''$ wide slits and the LRRed grism were used to cover the spectral range $5500\text{\AA} < \lambda < 9400\text{\AA}$ with an effective spectral resolution $R \sim 230$ at $\lambda = 7500\text{\AA}$. The spectroscopic targets were selected from the photometric catalogues using the VLT-VIMOS Mask Preparation Software (VVMPS; Bottini et al. 2005). The spectroscopic multi-object exposures were reduced using the VIPGI tool (Scodreggio et al. 2005; Zanichelli et al. 2005). Further details on observations and data reduction are given in Le Fèvre et al. (2004a,b).

The first-epoch data sample in the VVDS-F02 field extends over a sky area of $0.7 \times 0.7 \text{ deg}^2$ and has a median redshift of $z \sim 0.76$. It contains 7267 objects with secure redshifts (i.e. redshift determined with a quality flag ≥ 2), corresponding to an average sampling rate of 23% of the initial photometric sample. In our analysis we used the [OII] $\lambda 3727$ line and the 4000 \AA break as indicators of star formation activity and stellar ages respectively. As a consequence, we limited our sample to galaxies within the $0.5 \leq z \leq 1.3$ redshift interval, giving us a final number of 4277 galaxies, after removing spectroscopically confirmed QSOs and stars.

This sample provides an excellent laboratory to analyze spectral properties of galaxies at several redshift ranges, especially as it is accompanied by a wealth of photometric ancillary data, collected at several telescopes and described in the following papers: McCracken et al. (BVRI bands at CFHT, 2003); Radovich et al. (U-band at ESO-2.2m/WFI, 2004); *ubvrz* bands by the CFHT Legacy Survey project, McCracken et al. in prep.; (J and K_s at ESO-NTT/SOFI, Temporin et al. in prep., Iovino et al. 2005).

3. Methodology

In this section we will describe in some details the methodology adopted to obtain measurements of [OII] $\lambda 3727$ and $D_n 4000$ from

VVDS spectra and to derive estimates for specific star formation rates (SSFRs) and stellar masses.

3.1. Spectral measurements: [OII] and $D_n 4000$

Spectral features measurements have been obtained for all galaxies in our sample using the *platefit_vvds* software package. This software implements the spectral features measurement techniques described by Tremonti et al. (2004), but takes into account the lower spectral resolution of our data (for a detailed discussion see Lamareille et al. in prep.).

The two spectral measurements we use in this paper are the equivalent width of the [OII] $\lambda 3727$ doublet (EW[OII]) and the amplitude of the 4000 \AA break. In particular, we adopt the so-called narrow definition for the 4000 \AA break (hereafter $D_n 4000$), introduced by Balogh et al. (1999) and based on the ratio of the average spectral flux density in the bands 4050–4250 \AA and 3750 – 3950 \AA around the break. Compared to the original definition introduced by Bruzual (1983) the newly proposed index has the advantage of reducing the effect of dust reddening, because of the narrower portion of galaxy spectrum involved in the measurement (see for details Kauffmann et al. 2003a).

Comparing repeated observations for 140 objects in our sample, we estimated that the typical relative uncertainty affecting our measurements is $\sim 27\%$ and $\sim 10\%$ for the EW[OII] and $D_n 4000$, respectively. Moreover, given the typical signal-to-noise ratio of the spectra, we can estimate an average detection threshold for the [OII] doublet of approximately 8 \AA . Both this threshold and the measurement uncertainties depend somewhat on the galaxy redshift, as some fringing residuals contribute to increase the noise in the VVDS spectra in the wavelength range from 8200 to 9300 \AA .

3.2. Star Formation Rate Estimates

Adopting the formula proposed by Guzman et al. (1997) we can translate the EW[OII] in star formation rate estimates:

$$\text{SFR}(M_\odot \text{ yr}^{-1}) \approx 10^{-11.6-0.4(M_B-M_{B\odot})} \text{EW[OII]} \quad (1)$$

where we used the absolute magnitudes M_B as estimated in Ilbert et al. (2005). Although the average accuracy of the absolute spectrophotometric calibration of the VVDS sample is better than $\pm 10\%$ r.m.s., we favour the use of the EW[OII] instead of line fluxes to estimate the SFR. In this way we minimize the dependency of our estimates on bad weather conditions and slit losses (see for details Le Fèvre et al. 2005).

There are three main caveats for the reliability of the SFR conversion deduced using Eq. 1 from EW[OII] over the whole redshift interval ($0.5 \leq z \leq 1.3$): the uncertainty on the fraction of active galactic nuclei (AGN) present in our sample, the cosmic evolution of metallicity, and the amount of extinction.

One risk in interpreting line measurements as proxy for star-formation activity is the contamination arising from the presence of an AGN in the central region of a galaxy. In this case, the emission lines in the spectrum will be a mixture of contributions from both the AGN and star formation. While our sample does not contain the spectroscopically confirmed broad-line AGNs, it could be still contaminated by type II AGNs. We can estimate the fraction of type II AGN-dominated galaxies by using standard line ratios diagnostic tools, i.e. [OIII] $\lambda 5007/H\beta$ vs. [OII] $\lambda 3727/H\beta$ (see for details Lamareille et al. in prep.). The use of this diagnostic diagram is however limited to $z \leq 0.8$, because at higher redshift the required emission lines are out of the

observed wavelength range. In the redshift interval $z = 0.5 - 0.8$ approximately 7% of galaxies of our sample have an AGN identification in the standard line ratios diagnostics. The same fraction is found on the VVDS sample using new diagnostics among which $[\text{OII}]\lambda 3727$, $[\text{NeIII}]\lambda 3869$ and $\text{H}\delta$ in the redshift interval $0.9 < z < 1.3$ (Perez-Montero et al. in prep.) Therefore, we estimate the contamination from secure AGN-dominated galaxies in our final sample to be less than 7% between $z = 0.5$ and $z = 1.3$.

Another possible limitation we face in converting $\text{EW}[\text{OII}]$ into star formation estimates is related to the metallicity and its cosmic evolution, that could result into a systematic change of line intensities with redshift even if the star formation activity were to remain constant. Mouhcine et al. (2005) have shown that a variation of the metallicity by a factor of 4 can produce a variation of a factor of about 3 in the reddening-corrected $[\text{OII}]\lambda 3727/\text{H}\alpha$ flux ratio (see Fig. 12 in Mouhcine et al. 2005). This relation however has an opposite behavior for different metal regimes. In metal-poor (rich) galaxy population the $[\text{OII}]\lambda 3727/\text{H}\alpha$ flux ratio increases (decreases) with the metallicity. This subtle concept is important as low-mass galaxies ($< 10^{10} M_{\odot}$) are typically metal-poor ($0.2Z_{\odot}$), while massive galaxies ($> 10^{11} M_{\odot}$) are typically metal rich ($1.4Z_{\odot}$) (Gallazzi et al. 2005).

As for the direct effect of metallicity evolution on line strength, there is still considerable debate about the details of the evolution of the mass-metallicity relation. Savaglio et al. (2005) find very little change in metallicity for massive, already high-metallicity systems, up to $z \sim 1$. They find instead a significant overall increase of metallicity for low-mass, generally low-metallicity objects. Lamareille et al. (2006), on the contrary, observe a general decrease of metallicity which is essentially independent from galaxy mass, while the VVDS data (Lamareille et al. in prep.) show some indication of a smaller change of metallicity for low mass systems than for high mass ones. Overall these studies are concordant in finding an evolution of the metallicity within a factor of 2 up to $z \sim 1$. This would imply an uncertainty of less than a factor of two in our star formation rate estimates. As the observed variations in star formation activity discussed in Sect. 3.2 are significantly larger than this uncertainty, and the metallicity estimates we can obtain are highly uncertain too because of the low spectral resolution and low S/N of our spectra, we prefer not to correct our $[\text{OII}]$ measurements for metallicity variations.

Finally, we also have to consider the effects of dust extinction on our SFR estimates, although they are somewhat minimized by the use of equivalent widths instead of line fluxes. The observed line and continuum fluxes involved in the determination of the equivalent width are equally affected by the diffuse dust extinction within the galaxy, and the only differential effect would be due to localized extinction within HII regions, that should account for only a minor fraction of the total dust extinction within a galaxy (Kennicutt 1989). To account for the dust attenuation we corrected the $\text{EW}[\text{OII}]$ by the amount of the extinction provided by our template fitting using PEGASE (Fioc & Rocca-Volmerange 1997, see next section). The correction values obtained with this method vary within the interval $\text{EW}[\text{OII}]_{\text{corr}} / \text{EW}[\text{OII}] \in [1 - 2.7]$.

Apart from the caveats we already mentioned, for sake of completeness we could also add the possible uncertainties derived from the unknown physical condition of the ionizing gas and those related to the different sample used to calibrate $\text{H}\alpha/[\text{OII}]$ in Eq. 1 from the original one constituted by compact emission line galaxies (Guzman et al. 1997).

3.3. Stellar Mass Estimates

We obtain the stellar mass by fitting the photometric and spectroscopic data with a grid of stellar population synthesis models generated by the PEGASE2 population synthesis code (Fioc & Rocca-Volmerange 1999, astro-ph/9912179; Fioc & Rocca-Volmerange 1997), and using the GOSSIP Spectral Energy Distribution tool (Franzetti 2005). The models were produced assuming a Salpeter initial mass function (Salpeter 1955) to allow an easy comparison with previous analysis (e.g. Brinchmann & Ellis 2000; Fontana et al. 2004). The use of other prescriptions for initial mass functions does not introduce any significant difference in the redshift evolution of the mass estimate in the redshift interval explored (see Pozzetti et al. 2007). We use a set of delayed exponential star formation histories or "à la Sandage" (see Eq. 3 in Gavazzi et al. 2002) with galaxy ages, t , in the range from 0.1 to 15 Gyr, and star formation time-scales, τ , between 0.1 and 25 Gyr. Internal dust extinction is handled self-consistently with the star formation activity by the PEGASE2 code.

Stellar masses obtained with this method were compared with other estimates based on the fitting of the photometric data only and photometric plus spectroscopic data with Bruzual & Charlot (2003) models derived using different families of star formation histories. We find the various estimates to be consistent with each other in the investigated redshift interval. We estimate a statistical uncertainty on the mass computation of approximately 0.2 dex.

For the method adopted to construct the stellar mass function partitioned by the spectral classification explained in Sect. 3.4 and other technicalities we refer to Pozzetti et al. (2007) in which the total stellar mass function for the entire VVDS-F02 sample is presented. Here we briefly describe the most important points. We derive the mass function using the classical non-parametric $1/V_{\text{max}}$ formalism following Schmidt (1968) and Felten (1976) and a fit to the Schechter parameters. We take into account in the estimate of the mass function also the incompleteness resulting from non-targeted sources in our spectroscopic observations and for spectroscopic failure. The completeness in stellar mass, due to the magnitude limit of the sample (see discussion in Pozzetti et al. 2007) are $M_{\star} = 4.4 \times 10^9$, 8.9×10^9 , $2.5 \times 10^{10} M_{\odot}$ for $z \in [0.5 - 0.7]$, $[0.7 - 1]$, $[1 - 1.3]$, respectively.

Finally we derive a galaxy sample of 4048 objects with stellar masses $M_{\star} > 10^9 M_{\odot}$ over the redshift range covered by our investigation ($0.5 \leq z \leq 1.3$). We define the percentage of completeness in stellar masses below the mass limits by the ratio between number density observed and that obtained integrating the stellar mass function using the Schechter parameters. Our sample is complete in stellar mass down to $M_{\star} = 10^9 M_{\odot}$ at 95%, 85%, 74% for $z \in [0.5 - 0.7]$, $[0.7 - 1]$, $[1 - 1.3]$, respectively.

3.4. Spectral classification

To study the role played by the stellar mass in regulating the active phase of star formation, we adopt a parametric classification of galaxies based on the D_n4000 index used as an estimator of stellar ages (Hamilton 1985; Balogh et al. 1999).

We choose a value of $D_n4000 = 1.5$ to discriminate between *spectroscopic late-type* ($D_n4000 < 1.5$) and *spectroscopic early-type* ($D_n4000 > 1.5$) galaxies. Our choice is motivated both by galaxy evolution models and observations.

Single stellar population (SSP) models have shown that in a galaxy with solar metallicity experiencing an instantaneous burst of star formation, the spectrum of an underlying stellar

population reaches in 1 Gyr values of D_n4000 larger than 1.5 (Kauffmann et al. 2003a). Different results obtained using different stellar libraries are within the error of the D_n4000 measure (Kauffmann et al. 2003a; Le Borgne et al. 2006), while there is a possible dependency on metallicity for old stellar ages (>1 Gyr). Galaxies with values of metallicity as extreme as 0.05 (2.5) Z_\odot reach values of D_n4000 larger than 1.5 in 2.5 (0.8) Gyr after a burst (Kauffmann et al. 2003a). Le Borgne et al. (2006) investigate the D_n4000 evolution using other modes of star formation history. They show that the D_n4000 index reaches values larger than 1.5 after 1 Gyr from the initial activity also in galaxies with a period of constant star formation truncated 0.5 Gyr after the collapse, while galaxies with recurring bursts modes always keep the D_n4000 values below 1.5 in a period as long as 9 Gyr.

Observationally in the present-day galaxies, values of D_n4000 smaller (larger) than 1.5 have identified young (old) stellar populations with a separation between the two populations at 1 Gyr (Kauffmann et al. 2003b). This limit has been widely used in other observational studies (Miller & Owen 2002; Mignoli et al. 2005).

Hereafter we refer to our *spectroscopic early-* and *spectroscopic late-type* galaxies simply as early- and late-type galaxies, although the classification of a galaxy on color-, morphological-, spectroscopic-based scheme should be kept distinct. The different terminologies should not be mixed up, despite the robust trends existing among morphologies, colors, gas content, star formation activity, and other properties (for a recent review see Renzini 2006). The category of early-type galaxies, by virtue of their relatively simple star formation history, are generally used as the preferential category of objects to test galaxy formation and evolution and therefore one should be careful in the definition chosen to select them (see Franzetti et al. 2007).

4. Results

4.1. Evolution of Stellar Ages with Stellar Mass

In the local Universe there is a well established observational evidence that while young galaxies are preferentially low-mass systems, old galaxies are mostly massive systems. In particular, Kauffmann et al. (2003b) identify in their Fig. 2 the population of the first peak of the D_n4000 distribution observed at ~ 1.3 as emission line objects with a mean stellar age of 1 – 3 Gyr and low stellar mass ($< 3 \times 10^{10} M_\odot$). The second peak at $D_n4000 \sim 1.85$ corresponds instead to old (> 10 Gyr), massive ellipticals.

Figure 1 shows the histogram of D_n4000 distribution in different intervals of stellar masses and redshifts as indicated on the top and on the right respectively. For the VVDS-F02 data (rows 2–4) the histograms shown are corrected for non-targeted sources in our spectroscopic observations and for spectroscopic failures (the corrected total number and the actual number of observed galaxies are reported respectively in the first and second lines at the top of each panel).

To allow a direct comparison with the local Universe, the first row of Fig. 1 shows the D_n4000 distribution as derived from a local sample of SDSS DR4 galaxies within the same interval of stellar masses as ours (properly rescaled to account for the different IMFs). This plot enables us to explore the presence of any relation between stellar ages and stellar masses in the distant Universe. The vertical dotted lines represent the cutoff at $D_n4000=1.5$ adopted to sub-divide our objects in early- and late-types, as described in the Sect. 3.4. The vertical dashed line

Table 1. D_n4000 MEDIAN DISTRIBUTION

z	$10^{9-9.5} M_\odot$	$10^{9.5-10} M_\odot$	$10^{10-10.5} M_\odot$	$10^{>10.5} M_\odot$
~ 0	1.24 ± 0.00	1.28 ± 0.00	1.46 ± 0.00	1.68 ± 0.00
0.5 – 0.7	1.18 ± 0.01	1.20 ± 0.01	1.27 ± 0.01	1.52 ± 0.02
0.7 – 1.0	1.13 ± 0.01	1.16 ± 0.01	1.21 ± 0.01	1.37 ± 0.01
1.0 – 1.3	1.07 ± 0.04	1.07 ± 0.02	1.09 ± 0.01	1.25 ± 0.02

NOTES: D_n4000 median values in four intervals of stellar mass and three redshift bins for our VVDS-F02 sample. The error quoted in each interval represents the error on the median distribution using a statistical Jackknife technique. The median values of the D_n4000 distribution in a nearby galaxy sample (SDSS DR4) are also listed.

in each panel is the median of the D_n4000 distribution in that particular stellar mass interval and redshift bin (see Tab. 1).

The first evidence shown by Fig. 1 is the different behavior of the D_n4000 distribution for the four bins of stellar mass, evidencing a clear dependency of the stellar age on stellar mass that holds at all epochs up to $z \sim 1.3$. Even at the highest redshift bin investigated the D_n4000 distributions follow closely the behavior observed in the local Universe. Low mass galaxies have small D_n4000 values and, as mass increases, the galaxy distribution moves to larger D_n4000 values. At any fixed redshift bin, the relative abundance of early-type galaxies ($D_n4000 > 1.5$) increases as mass increases. The largest D_n4000 values, and thus the oldest underlying stellar populations, are hosted in the most massive galaxies at all redshifts up to $z \sim 1.3$.

Another striking evidence coming from Fig. 1 is that for the lower mass galaxies ($< 10^{10} M_\odot$) the shape of the D_n4000 distribution does not seem to evolve with time between $z \sim 1$ and $z \sim 0$. For these galaxies the D_n4000 distribution is extremely peaked around $D_n4000 \sim 1.1$ in all redshift bins, suggesting a good correspondence up to high redshifts between a low stellar mass and a young underlying stellar population. Vice-versa galaxies in the highest stellar masses bins we explore populate both early- and late-type galaxies regions in the D_n4000 distribution and do show significant evolution with redshift. For these stellar mass bins as cosmic time goes by galaxies populate progressively the locus of larger D_n4000 values and a secondary peak emerges in the D_n4000 distribution. The gradual accumulation of the secondary peak is a process started at early epochs ($z > 1.3$) that continues efficiently down to the local Universe.

Our findings on the distribution of the stellar ages and stellar mass can be interpreted in the framework of a top-down picture of the stellar mass assembly history of galaxies, or, as it is termed, “archaeological downsizing” following Neistein et al. (2006), see also Thomas et al. (2005); Cimatti et al. (2006); Bundy et al. (2006). Evidence of this top-down stellar mass assembly is already present in literature. Studies on stellar age, metallicity, and cosmic star formation at $z \sim 0$ prove that stars in massive galaxies were formed long ago and over a short period of time (e.g. Thomas et al. 2005; Heavens et al. 2004; Jimenez et al. 2005). At high redshifts the reddest galaxies already possess old ages (> 1 Gyr), establishing their formation epoch at $z > 2$ (McCarthy et al. 2004; Cimatti et al. 2004). Furthermore, massive proto-disk galaxies already exist at $z \sim 2 - 3$ (e.g., Labbé et al. 2003; Stockton et al. 2004; Förster Schreiber et al. 2006; Genzel et al. 2006). On the con-

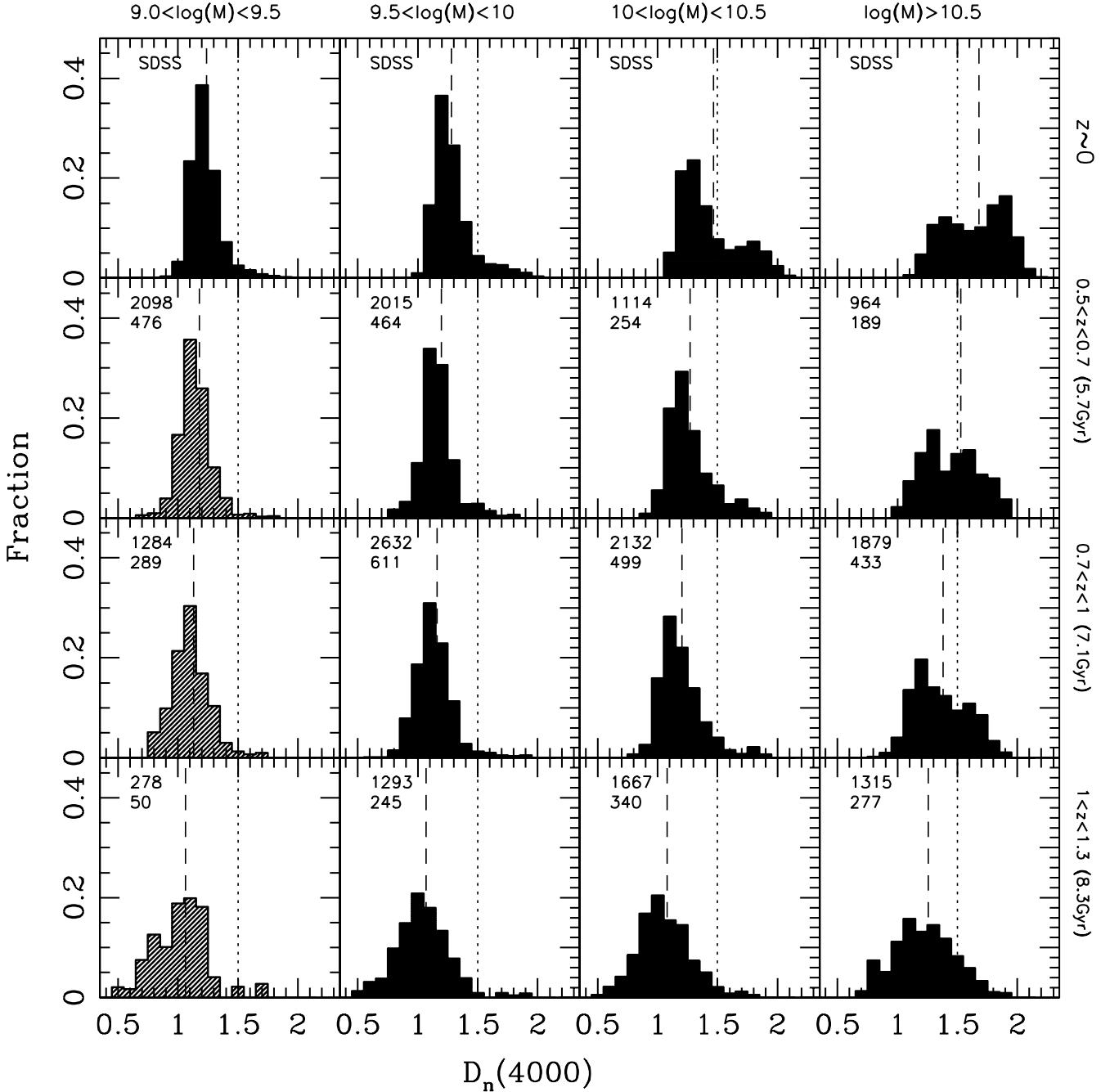


Fig. 1. Histograms showing the fraction of VVDS-F02 galaxies as a function of $D_n(4000)$ in four different ranges of stellar mass and in three redshift bins ($0.5 - 0.7$, $0.7 - 1.0$, $1.0 - 1.3$, rows 2-4). We plot as a comparison in the first row the $D_n(4000)$ galaxy distribution for the local Universe ($z \sim 0$) from the SDSS DR4. The counts corrected for non-targeted sources in our spectroscopic observations and for spectroscopic failures (unidentified sources) following Ilbert et al. (2005) are reported in the first line at the top of each panel, the observed counts of galaxies in the second line. The vertical dotted lines at $D_n(4000) = 1.5$ represent the adopted separation between early- and late-type galaxies. The vertical dashed lines represent the median $D_n(4000)$ distribution in each panel. Panels with 100% mass completeness have full-shaded $D_n(4000)$ distribution, while the light-shaded histograms at $M = 10^{9-9.5} M_\odot$ are mass complete at 95%, 85%, 74% for $0.5 \leq z \leq 0.7$, $0.7 \leq z \leq 1$, and $1 \leq z \leq 1.3$, respectively, as computed integrating the mass function using the Schechter parameters (see Pozzetti et al. 2007).

trary, the underlying stellar ages of late-type galaxies apparently do not show evolution. This observation is probably justified by a continuous and efficient formation rate of new stars (see next

Sect. 4.3) as discussed also in other studies (Arnouts et al. 2007, Faber et al. 2006).

Our sample shows to which extent the stellar mass drives the galaxy evolution. For the first time we present a direct comparison of stellar ages and stellar masses of galaxies over the last 8 Gyr extending the seminal work by Kauffmann et al. (2003b) on nearby galaxies.

4.2. SFR dependence on stellar mass and redshift

A cosmic decline of the star formation activity has been presented in several studies, starting from field redshift surveys by Lilly et al. (1996); Madau et al. (1996). Nowadays, the knowledge of the cosmic star formation history out to redshift ~ 1 is quite profound (Hopkins & Beacom 2006, and references therein). However many aspects of galaxy evolution, like the contribution to galaxy mass assembly of various categories of galaxies still need to be understood (see for details Cimatti et al. 2006).

Figure 2 (panel a) shows the median distribution of EW[OII] interpreted as proxy for the star formation activity for our entire galaxy sample in the redshift interval $z = 0.5 - 1.3$ as a function of the stellar mass. The star formation activity has a clear mass-based evolution and shows the well-established global star formation rate decline. Generally, at a given redshift bin the smaller the stellar mass of the galaxy, the more actively it is forming stars.

These results obtained over the redshift interval covered by our sample are in excellent agreement with the findings by Feulner et al. (2005a) based on a large photometric redshift sample of 9000 galaxies from the FORS Deep Field and the GOODS-S field. Feulner et al. (2005a) show a similar trend for the SSFRs at different stellar mass intervals with no contribution to the stellar mass growth for massive galaxies (cf. Fig. 2 in Feulner et al. 2005a). We also find an excellent agreement in the common redshift range with the study of 207 galaxies from the spectroscopic GDDS. Juneau et al. (2005) show that massive GDDS galaxies ($> 10^{10.2} M_{\odot}$) are in a quiescent mode, and lower mass GDDS galaxies in a burst phase.

Our results, being obtained on large spectroscopic sample put on firmer grounds the results found in photometric galaxy catalogues and relatively smaller spectroscopic surveys: the star formation in early-type galaxies and in general in massive systems is at very low values since $z \sim 1 - 1.3$.

In Fig. 2 (panel b and c) we plot the median EW[OII] distribution in early- and late-type galaxies separately. These figures show that both massive, early- and late-type galaxies have negligible levels of star formation. Vice-versa low-mass, early-type galaxies, although possessing an old underlying stellar population on the basis of their spectroscopic classification, show a high value of the star formation activity, comparable or even higher than the most active late-type systems (blue line in Fig. 2.c). This result holds over the entire redshift range explored. Furthermore the EW[OII] strength of these objects dramatically increases as a function of the redshift. However, we will show in Fig. 4 that this category of objects represents only a minor fraction ($< 5\%$) of the population of galaxies at that redshift and stellar mass interval and one should exercise caution in the interpretation of this result as this population is the most affected by mass incompleteness. Early-type galaxies with low-level of star formation activity are under-estimated with the consequence to weigh more those with relatively larger EW[OII], thus we avoid to use the values of the highest redshift bin.

In the recent years a number of studies have pointed out a contamination on the order of 20% up to 50% of the red (color-selected) population from star forming galaxies

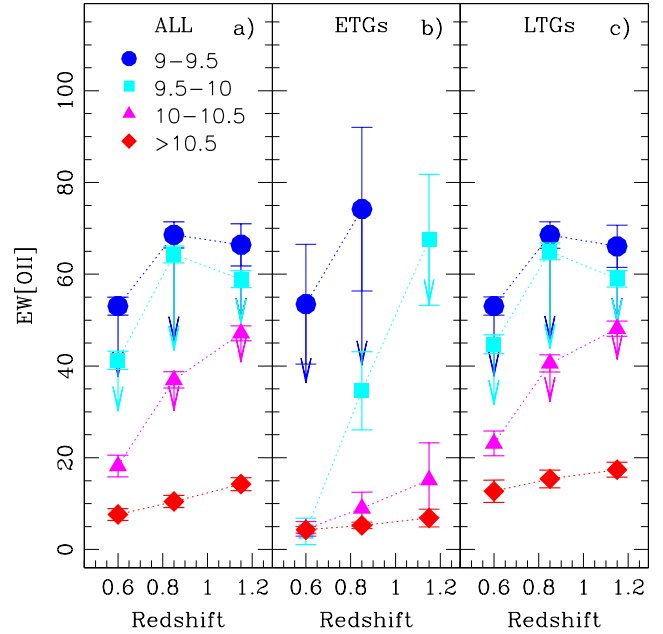


Fig. 2. The median EW[OII] as a function of the redshift for our VVDS-F02 sample (a) in bins of stellar masses, coded as follow: $9.0 < \log(M) \leq 9.5 M_{\odot}$ (blue, circle), $9.5 < \log(M) \leq 10 M_{\odot}$ (cyan, square), $10 < \log(M) \leq 10.5 M_{\odot}$ (magenta, triangle), $\log(M) > 10.5 M_{\odot}$ (red, diamond). The same visualization is presented for the spectroscopic early- (b) and late-type galaxies (c). The filled symbols represent the EW[OII] corrected for dust extinction, and the arrows the corrections applied.

(Strateva et al. 2001; Franzetti et al. 2007; Cimatti et al. 2002; Kriek et al. 2006). It is also known in literature that the abundance of objects classified as early-types with a non negligible rate of star formation is increasing with redshift (Tresse et al. 1999). The contaminating systems are constituted by a mixture of galaxies with dusty star-burst properties and galaxies that for internal, physical mechanisms are morphologically classified later than Sa. As a direct consequence of our adopted classification the number of quiescent galaxies with properties in common with star forming galaxies (5%) is definitively a lower fraction compared to previous studies (20-50%) that rely on morphology and color classifications. For example thanks to our classification criterion reflecting the age of the underlying stellar population we correctly classify populations of galaxies like dusty-star forming EROs. They possess in fact red colors but low D_n4000 values (Mignoli et al. 2005) which make them misclassified in any classification relying on colors.

The general picture which emerges from the Figs. 1 and 2 follows the classical concept of downsizing as firstly suggested by Cowie et al. (1996). In this framework one expects a continuous growth with time of low mass galaxies while the massive galaxies have completed their growth at early epochs. This galaxy attitude is also termed downsizing in time (Neistein et al. 2006). Additional evidences supporting the downsizing scenario in time come from the results based on different studies on the mass and luminosity functions, the global and specific star formation rates (e.g., Bauer et al. 2005; Juneau et al. 2005; Feulner et al. 2005a,b; Tresse et al. 2006).

One another important aspect becomes apparent when comparing the results summarized in Figs. 1 and 2. One knows that the D_n4000 strength is the result of the cumulative star formation history of a galaxy. Instead the [OII] line is sampling only the instantaneous star formation activity, because the ionizing flux in HII regions is provided almost entirely by massive stars ($\log(M) > 10M_\odot$) with lifetimes limited to 20 Myr or less. As already discussed in Sect. 3.4, D_n4000 values below 1.5 are indicative of significant star formation activity within the last 1 Gyr, while values above 1.5 are associated to galaxies that have finished forming their stars, at least 1 Gyr ago, and are therefore evolving mostly, if not exclusively, via the passive evolution of their stellar population. Therefore, the star formation time-scales probed with the D_n4000 and the [OII] equivalent width are very different.

In our sample, we observe that massive galaxies are the only subset of the population to show a significant presence of objects with large D_n4000 , and all these objects have, at the same time, very low or null star formation activity. Both indicators (D_n4000 and $EW[OII]$) are consistently pointing towards a star formation history peaked in the past for these massive galaxies, with little or no residual star formation taking place at the epoch of the observation. Most of the low mass systems show just the opposite characteristics. Almost all galaxies in this subset have small D_n4000 and a rather strong current star formation activity. The indicators suggest a general picture of extended star formation activity, that makes these objects dominated by the young stellar population at all epochs (although with this kind of analysis we cannot say anything about their epoch of formation, of course). Finally, despite their different time-scales both indicators shows the same connection between stellar mass and star formation history. We need to note, however, that among the low mass systems a small fraction of objects possess the two star formation indicators which are not in agreement. In fact we see from Fig. 2 that there exists a population of spectral early-type galaxies where a large D_n4000 value, that points towards a predominantly old stellar population, is coupled with a significant [OII] emission, indicative of ongoing star formation activity. However, as we discussed earlier, the impact of this galaxy category on the entire galaxy population is negligible. The very good agreement observed for massive objects between the instantaneous and the integrated star formation indicator can be understood assuming that the dominant mode of star formation activity for these systems is a continuous one, with relatively smooth variations in time, and with no significant contribution from strong bursts. A similar conclusion has been presented recently by Noeske et al. (2007), based on their analysis of the AEGIS survey data. For smaller mass objects, instead, star-bursts must become more important, and they can easily explain the presence of a fraction of galaxies for which the instantaneous and integrated star formation indicators are not in agreement. We notice that a somewhat similar dependence of burst activity on galaxy stellar mass has been observed in the SDSS data by Kauffmann et al. (2003a), although their most recent work (Kauffmann et al. 2006) indicates an important role for galaxy surface mass density more than for total mass in regulating star formation activity.

4.3. Stellar Mass Assembly in Early- and Late-Type Galaxies

We show in Fig. 3 the stellar mass function in three redshift bins both for early- and late-type galaxies according to the spectral classification introduced in Sect. 3.4. The parameters of the Schechter fit (α , M_{star}^* , ϕ^*) for early- and late-type galaxy samples are listed in Tab. 2 along with their uncertainties. We fix the

slope of the highest redshift bin to the slope value as determined in the interval $0.7 \leq z \leq 1$ where it is better constrained. The vertical dashed line in each panel represents our mass completeness in that redshift bin (see Sect. 3.3). To judge the evolution in the three redshift intervals we over-plot the Schechter fits to early- and late-type stellar mass functions of the lowest redshift bin at each panel. To have a direct comparison with previous results found in the literature we also plot in Fig. 3 the type-dependent stellar mass obtained in the DEEP2 (Bundy et al. 2006) properly rescaled to the Salpeter IMF. We also plot the results from the K20 (Fontana et al. 2004), in which early- and late-type galaxies are computed using a similar criterion. They are calculated however in slightly different redshift bins ($0.2 \leq z \leq 0.7$ and $0.7 \leq z \leq 1.3$).

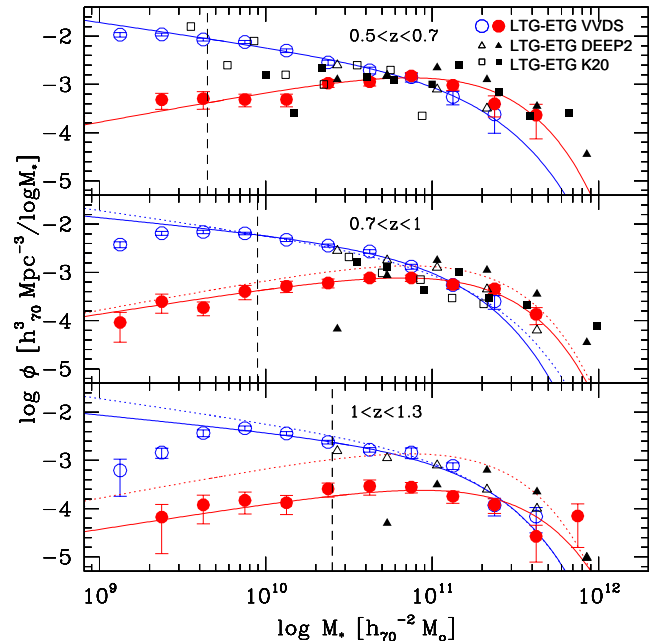


Fig. 3. Stellar mass function for the spectroscopically classified late-type (empty circles) and early-type (filled circles) galaxies from VVDS-F02 sample. Results for spectral type galaxies from K20 survey by Fontana et al. (2004) and for color-based type galaxies from DEEP2 survey (Bundy et al. 2006) are also over-plotted by square and triangle symbols, respectively. The completeness limits computed integrating the mass function using the Schechter parameters, are 95%, 85%, 74% at $z = 0.5 - 0.7, 0.7 - 1, 1 - 1.3$ for the stellar mass interval $\log(M)=9-9.5$, while nearly 98% for stellar masses below the full (100%) complete limits (the vertical shaded lines).

In general from Fig. 3 we observe up to $z \sim 1$ only a mild or even no evolution in the stellar mass function for both spectral type galaxies. At $z > 1$ a stronger evolution in the stellar mass function occurs for early-type galaxies, while late-type galaxies evolve only mildly, in particular at the massive tail. We note, moreover, that the massive end of the mass function is mainly dominated by early-type galaxies up to redshift $z \sim 1$, and for stellar mass larger than 2.5×10^{11} most of the galaxies have an early-type classification even up to $z = 1.3$. Late-type galaxies mostly contribute to the low-mass part of the mass function at all redshifts.

Table 2. SCHECHTER FIT PARAMETERS

z range		α	$\log M_{star}^*$ ($h_{70} M_{\odot}$)	ϕ^* ($10^{-3} h_{70}^3 Mpc^{-3}$)		α	$\log M_{star}^*$ ($h_{70} M_{\odot}$)	ϕ^* ($10^{-3} h_{70}^3 Mpc^{-3}$)	M_{tr}
$0.5 < z < 0.7$	ETG	$-0.36^{+0.19}_{-0.20}$	$11.06^{+0.12}_{-0.12}$	$1.50^{+0.25}_{-0.30}$	LTG	$-1.50^{+0.11}_{-0.09}$	$11.10^{+0.27}_{-0.21}$	$0.75^{+0.5}_{-0.35}$	10.87
$0.7 < z < 1.0$		$-0.46^{+0.20}_{-0.19}$	$11.09^{+0.12}_{-0.10}$	$0.80^{+0.30}_{-0.15}$		$-1.34^{+0.14}_{-0.12}$	$10.96^{+0.13}_{-0.13}$	$1.30^{+0.5}_{-0.45}$	11.11
$1.0 < z < 1.3$		-0.46	$11.20^{+0.07}_{-0.06}$	$0.25^{+0.15}_{-0.15}$		-1.34	$11.08^{+0.07}_{-0.08}$	$0.75^{+0.1}_{-0.10}$	11.42

NOTES: The listed values are computed on the early-type (ETG) and late-type (LTG) samples using a classification scheme based on the age-estimator D_n4000 (see Sect. 3.4).

The overall picture emerging from our stellar mass function with an increasing (decreasing) relative contribution of early (late) type galaxies with increasing mass and cosmic time agrees quite well with previous results (e.g. Fontana et al. 2004; Bundy et al. 2006). Generally the stellar mass function of late-type galaxies agrees very well in all studies. As far as the stellar mass function for the early-type galaxies is concerned the better agreement is obtained with the study by Fontana et al. (2004) which use as well a spectral classification, instead of a rest-frame color scheme (Bundy et al. 2006). A slightly worse concordance is found for the early-type galaxy densities at $z > 0.7$ with Bundy et al. which are larger than the one computed in our study (cf. filled triangle with filled circle in Fig. 3).

As only a mild evolution in the overall stellar mass function is observed in our sample at least up to $z \sim 1.2$ (Pozzetti et al. 2007), Fig. 3 shows a redistribution of the stellar mass amongst the spectral types with a declining contribution to the overall mass function of massive late-type with time associated with an increasing fraction of massive early-type galaxies.

The redistribution of galaxy types was reported by Brinchmann & Ellis (2000) computing the stellar mass density in a small sample of I-selected galaxies with spectroscopic redshifts and infrared photometry. Using Hubble Space Telescope morphologies, Brinchmann & Ellis (2000) observed a decline in the mass density of irregular galaxies from $z \approx 1$ to today either associated to a transformation into regular morphologies and/or to merging mechanisms. These results were confirmed by Bundy et al. (2005) using a sample of approximately two thousand morphologically-classified galaxies from GOODS (Giavalisco et al. 2004). Later on Bundy et al. (2006) provide further supports to the stellar mass redistribution using the DEEP2 spectroscopic sample producing type-dependent stellar mass functions based on rest-frame colors. Further evidence can be found also in other studies, for example, a similar modest change in abundance of massive early-type up to $z \sim 1$ was found in the K20 sample which has a high redshift accuracy and a spectral classification similar to ours (Fontana et al. 2004). The constancy in blue populations and the increasing trend of the red sequence classified according to $(NUV - r)$ colors have been observed in a study of stellar mass density by Arnouts et al. (2007), and observed previously by Borch et al. (2006); Martin et al. (2007).

We observe in Fig. 3 a downward transition with time of the threshold in the stellar mass above which one category of objects becomes dominant in the relative contribution to the total stellar mass function. This characteristic mass, or transition mass (M_{tr} reported in Tab. 2), was detected in the local Universe around $3 \times 10^{10} M_{\odot}$ (Kauffmann et al. 2003b; Baldry et al. 2004). Bundy et al. (2006) report its evolution with cosmic time using three different methods to define the two galaxy categories: galaxies are partitioned according to rest-frame colors, to the star

formation rate and to morphological properties. Our findings are in between those obtained dividing by colors and by morphology in Bundy et al. (2006). We find a similar trend in cosmic time when comparing their crossovers obtained using galaxy morphologies and colors with our results based on the D_n4000 index, while a less steeper evolution is observed when considering the classification obtained with the SFR indicator.

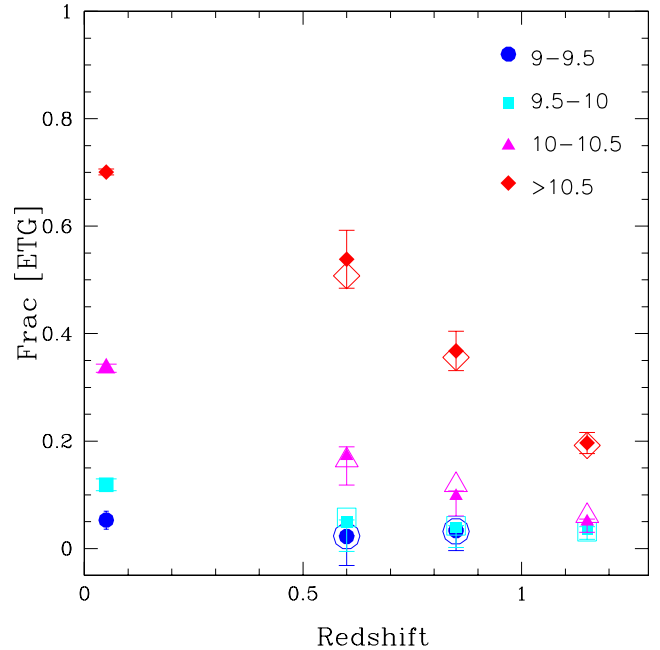


Fig. 4. The evolution of the fraction of galaxies classified as spectroscopically early-type in different mass intervals. The mass bin is coded as follows: $9.0 < \log(M) \leq 9.5 M_{\odot}$ (blue, circle), $9.5 < \log(M) \leq 10 M_{\odot}$ (cyan, square), $10 < \log(M) \leq 10.5 M_{\odot}$ (magenta, triangle), $\log(M) > 10.5 M_{\odot}$ (red, diamond). Filled symbols represent the counts of observed galaxies, while the open symbols represent the counts corrected for statistical weights (see text). The points at $z \sim 0$ are our SDSS reference points.

To show the differential evolution of galaxies and the general redistribution in stellar mass among galaxies we plot in Fig. 4 the evolution of the early-type galaxy fraction over the entire (early- and late-type) population for different stellar mass bins as a function of redshift. Both statistically-weighted corrected counts and observed counts are used in the computation and plotted with different symbols. The error-bars include both the uncertainties

in the spectral measurements and the effect of changing the classification threshold due to the D_n4000 errors. As in Fig. 1 we report the reference points at $z \sim 0$ from a local galaxy sample (SDSS DR4).

The relative evolution of the abundances of galaxies depends strongly on galaxy stellar mass. This is shown for the early-type galaxies in Fig. 4 where the relative fraction of the most massive galaxies of this category significantly changes with cosmic time. The strong evolutionary trend is emphasized by the lack of evolution in the abundances with time of the massive late-type galaxies. This is not the case for the less massive population (10^9 – $10^{10} M_\odot$) for which its relative abundance does not evolve significantly with time. In fact both early- and late-type categories evolve accordingly and the number density of low-mass early-type galaxies is very small (Fig. 3).

As the VVDS is a magnitude limited survey, we have to remind that we start to become incomplete at lower masses for higher redshifts. On the other hand as the galaxies that start to drop out from the sample are preferentially early-type galaxies that contribute little to the low mass bin (see Figs 1 and 3) the total effect on Fig. 4 is small. Furthermore, we obtained similar relative abundances and trend with redshift using the $1/V_{max}$ statistic as well as the Schechter fit extrapolated below the completeness limit. Therefore, the general trend observed in the less massive galaxies can not be totally justified by our incompleteness and our results remain solid.

To summarize our results suggest a galaxy mass assembly history with a mild total evolution with redshift in number density (Pozzetti et al. 2007) in particular for very massive galaxies ($> 2.5 \times 10^{11} M_\odot$), which are constituted mainly by early-type galaxies up to the redshift sampled ($z < 1.3$). Since the relative fraction of massive ($> 10^{10.5} M_\odot$) early- and late-type galaxies evolves with cosmic time we witness a spectral transformation of late-type systems into old massive galaxies at lower redshift. In the following we analyze the efficiency of this mass assembly process driven by the star formation rate observed in late-type galaxies.

4.4. Efficiency in the Stellar Mass Assembly Process

In the hypothesis of dry merging - merging of quiescent galaxies without gas (star formation) involved - the age of the galaxy (i.e. the time elapsed since it assembled its current stellar mass) may not coincide with the age of its underlying stellar population. As a consequence the processes of star formation and mass assembly remain distinct: it is possible that stars which formed long ago were assembled only recently in a newly created galaxy (Renzini 2007; Cimatti et al. 2006; Bundy et al. 2006). Within such a scenario one should also consider two separate downsizing signatures, i.e. downsizing in time (the transfer of star formation activity to lower mass galaxies) and archaeological downsizing (the fact that older stars are hosted by more massive galaxies). If one or more mechanisms allow for a quenching of star formation activity earlier in massive galaxies, and if dry mergers only represent a minor contribution to the galaxy mass assembly, then the two concepts of downsizing express one single idea.

To investigate this issue we look upon the efficiency in assembling stellar masses of galaxies and verify whether the amount of galaxy progenitors can justify the mass assembled without invoking any (dry) merger mechanism. We define for each galaxy at redshift z the time Δt as the time interval between the age of the Universe at the observed redshift z and the time corresponding to the lower limit of the redshift bin in which the

galaxy falls. For three redshift bins we plot with left-leaning diagonals (blue-coded) the D_n4000 distribution of galaxies which assemble enough stellar mass to move to a higher mass interval within a time Δt . The right-leaning diagonals (red-coded) represent the galaxies staying over the time Δt in the mass interval assigned at the time of the observations. The assumption is that these galaxies will sustain a constant observed SFR over the time Δt , which appears to be a reasonable assumption as our Δt is never larger than 1.3 Gyr.

Figure 5 shows that the lower the stellar mass the larger is the fraction of galaxies which can sustain a significant stellar mass growth, i.e. not only forming stars but effectively assembling mass. Once a galaxy reaches a certain stellar mass, it terminates to grow efficiently. The physical reason could be the natural exhaustion of the gas reservoir contained in massive galaxies which did consume it efficiently in the first phase of their life. On the contrary, low-mass galaxies having sustained over the time a lower rate of star formation activity still have a certain amount of fueling.

This characteristic stellar mass at each redshift tells us when a galaxy population stops to accumulate a significant amount of new stellar mass. Its evolution with cosmic time parallels that of the quenching mass, defined as the mass at which no active systems are observed (see for details Bundy et al. 2006). Galaxies show in fact a general decline in the mass assembly efficiency from high to low redshifts and low-mass systems appear to be able to grow significantly in stellar mass down to very low redshifts, while the majority of early-type galaxies at any stellar mass is largely inefficient in increasing its stellar mass.

These results and those obtained in previous sections support the hypothesis of apparent no evolution in the blue sequence proposed by Faber et al. (2005) and the mild evolution of the early-type class of galaxies (Zucca et al. 2006; Brown et al. 2007, Arnouts et al. 2007) which are largely inefficient at assembling mass at all epochs (at least since $z \sim 1.3$), and are progressively decreasing their efficiency as cosmic time progresses. In particular, on the basis of the mass migration from blue to red objects, Arnouts et al. (2007) propose a similar time-scale for the period required for blue galaxies to quench their star formation activity and move to the red sequence, and the birth rate time of blue galaxies which are continuously refilled by new stars.

If we consider the galaxies with stellar mass M_i ($M_{i=1,2,3,4} = 9 - 9.5, 9.5 - 10, 10 - 10.5, > 10.5$) observed at redshift z_j ($z_{j=1,2,3} = 0.5 - 0.7, 0.7 - 1, 1 - 1.3$), their progenitors are the sum of two galaxy contributions if no merging activity is advocated. The first progenitor class is constituted by galaxies with mass M_{i-1} at z_{j-1} that are assembling enough stellar mass to migrate in the higher mass interval within a time Δt , where Δt was previously defined. The second contributors are galaxies with stellar mass included in the same mass interval (M_i) at the epoch z_{j-1} that in a time Δt are not growing sufficient mass to flow in the subsequent stellar mass interval.

We compute within our mass completeness limit the number (per unit of co-moving volume) of galaxies observed at redshift z_j of stellar mass M_i and that of progenitors at redshift z_{j-1} as described above. We obtain that the number of progenitors at z_{j-1} can account, on average, for $80\% \pm 10\%$ of the galaxies at z_j of stellar mass M_i . This percentage is actually close to 100% for the most massive galaxies. This result shows a good agreement between the evolution of stellar mass function and that of the star formation activity up to $z \sim 1$, and therefore that no significant contribution to the mass assembly process is required from merging activity. A similar conclusion has been presented recently by Bundy et al. (2007) by comparing the dy-

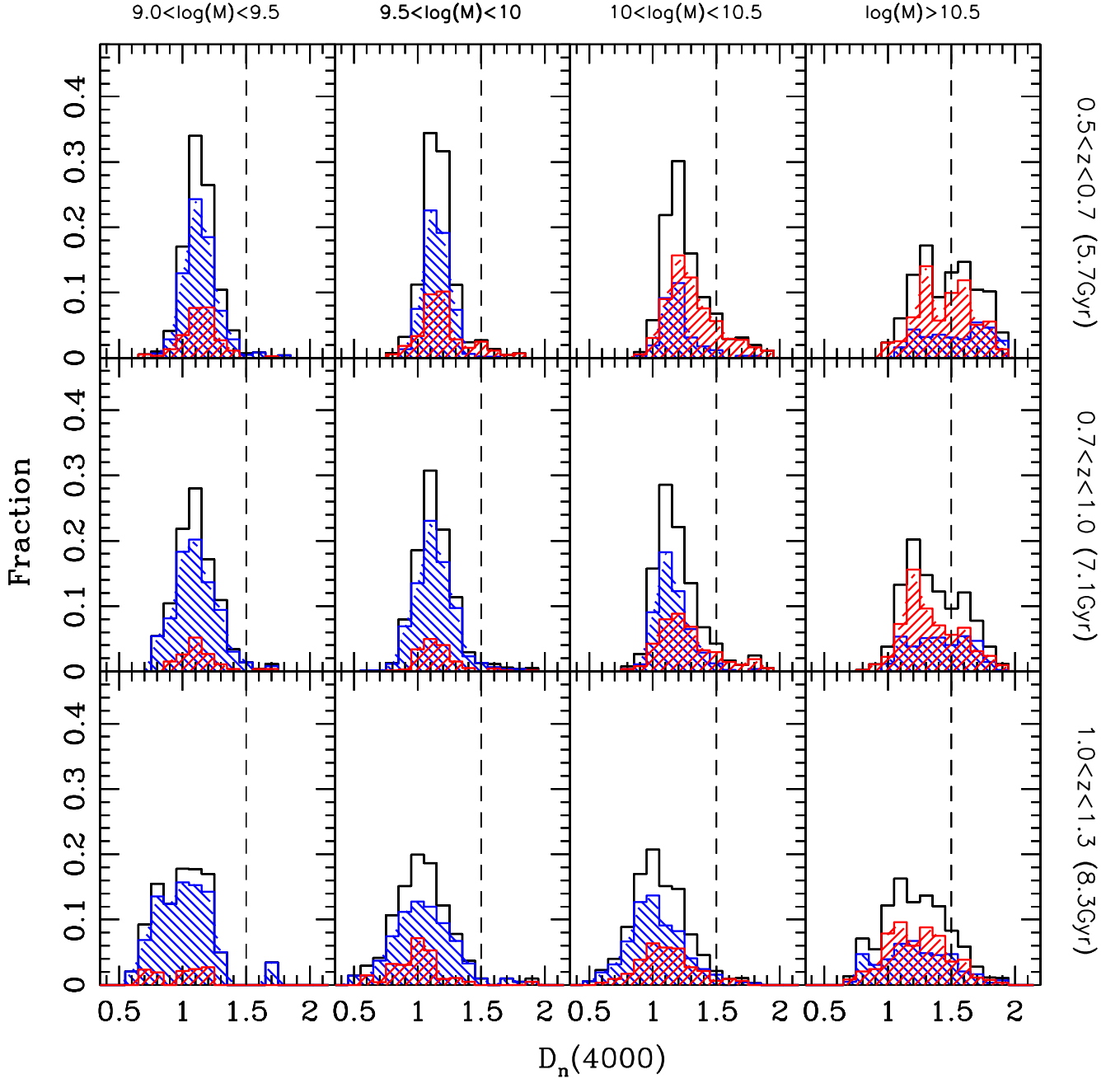


Fig. 5. Histograms showing the fraction of VVDS galaxies as a function of $D_n(4000)$ for four different ranges of stellar mass at three redshift epochs ($0.5 - 0.7$, $0.7 - 1.0$, $1.0 - 1.3$). The corresponding look-back time is also indicated. We define Δt for each galaxy at redshift z as the time interval between the age of the Universe at the observed redshift z and the time corresponding to the lower limit of the redshift bin in which the galaxy falls. Left-leaning diagonal (blue) histograms represent those galaxies that assemble within a time Δt a stellar mass enough to move to a higher mass interval and with right-leaning diagonals (red) those staying in the mass interval assigned at the time of the observations. The assumption is that these galaxies will sustain a constant observed SFR over the time Δt , which turns to be a reasonable assumption as our Δt is never larger than 1.3 Gyr.

namical and stellar mass of spheroidal galaxies in the GOODS fields. Should this scenario here described turn out to be correct it would imply that the all recent observations on galaxy evolution can be summarized with one single concept of downsizing. Still, a more detailed and quantitative analyses of the mass function evolution is needed before a more accurate evaluation of the role played by mergers in the build up of the galaxy mass

can be obtained. It is in fact well known that mergers do take place and recently individual cases of dry merger have also been listed by e.g., Bell et al. (2006); Tran et al. (2005). We cannot therefore exclude the possibility that between two redshift bins a fraction of galaxies moves from mass bin M_i to a higher mass bin via merger, although this merging activity would have to satisfy

rather tight constraints in order to preserve the observed distribution of stellar masses and ages.

5. Summary

We investigated the relationship between galaxy stellar age and stellar mass as a function of redshift in a mass-complete spectroscopic sample selected from the VIMOS VLT Deep Survey (VVDS). Up to $z \sim 1.3$ we confirmed the presence of a relationship mass-stellar ages that parallels the one observed in the local Universe (see Kauffmann et al. 2003b). In all redshift bins explored, low mass galaxies ($< 10^{10} M_{\odot}$) are dominated by a young stellar population, as witnessed by the low D_n4000 values. For higher mass galaxies ($> 10^{10} M_{\odot}$), on the contrary, the percentage of galaxies dominated by an old stellar population grows regularly with cosmic time. This process is more efficient the higher is the galaxy stellar mass considered. This result supports the so-called ‘archaeological downsizing’: the stellar population in massive galaxies formed at earlier times than the one in low-mass galaxies.

We then explored SFR evolution as a function of stellar mass. The percentage of quiescent galaxies, as witnessed by their low EW[OII] values, increases when moving to lower redshifts and higher masses. This trend is clearly visible both for galaxies with a young stellar population and for galaxies with a old stellar population. The emerging picture is one where low mass galaxies ($< 10^{10} M_{\odot}$) are subject to bursts of star formation activity up to recent times, while the dominant mode of star formation for massive galaxies ($> 10^{10} M_{\odot}$) is a smooth one, with no significant contributions from strong bursts. Therefore not only the bulk of the stellar population in massive galaxies formed at earlier times but the location where the mass gets assembled more efficiently at each redshift moves to lower mass galaxies with cosmic time.

We have also shown a mild total evolution with redshift of mass assembly history, in particular for the very massive galaxies ($> 2.5 \times 10^{11} M_{\odot}$) which are mainly early-type objects, up to highest sample redshift ($z \sim 1.3$). Since the relative fraction of massive ($> 10^{10.5} M_{\odot}$) early- and late-type galaxies evolves with cosmic time we are witnessing a spectral transformation of late-type systems into old massive galaxies at lower redshift.

Finally when we consider the joint distribution of stellar mass and star formation activity to quantify the efficiency with which galaxies assemble their stellar mass, we obtain a scenario where it is possible to account for the number of passively evolving galaxies up to $z \sim 1$ without invoking any (dry) merging mechanism. Our observations well agree with a scenario where not only the stellar population in massive galaxies formed earlier than the one in low-mass galaxies, but massive galaxies themselves were the first to be assembled.

6. Acknowledgments

This research has been developed within the framework of the VVDS consortium. This work has been partially supported by the CNRS-INSU and its Programme National de Cosmologie (France), and by Italian Ministry (MIUR) grants COFIN2000 (MM02037133) and COFIN2003 (num. 2003020150). The VLT-VIMOS observations have been carried out on guaranteed time (GTO) allocated by the European Southern Observatory (ESO) to the VIRMOS consortium, under a contractual agreement between the Centre National de la Recherche Scientifique of France, heading a consortium of French and Italian institutes, and ESO, to design, manufacture and test the VIMOS

instrument. DV acknowledges the support through a Marie Curie ERG, funded by the European Commission under contract No. MERG-CT-2005-021704. Based on observations obtained with MegaPrime/MegaCam, a joint project of CFHT and CEA/DAPNIA, at the Canada-France-Hawaii Telescope (CFHT) which is operated by the National Research Council (NRC) of Canada, the Institut National des Science de l’Univers of the Centre National de la Recherche Scientifique (CNRS) of France, and the University of Hawaii. This work is based in part on data products produced at TERAPIX and the Canadian Astronomy Data Centre as part of the Canada-France-Hawaii Telescope Legacy Survey, a collaborative project of NRC and CNRS.

References

- Baldry, I. K., Glazebrook, K., Brinkmann, J., et al. 2004, *ApJ*, 600, 681
 Balogh, M. L., Morris, S. L., Yee, H. K. C., Carlberg, R. G., & Ellingson, E. 1999, *ApJ*, 527, 54
 Bauer, A. E., Drory, N., Hill, G. J., & Feulner, G. 2005, *ApJ*, 621, L89
 Bell, E. F., Naab, T., McIntosh, D. H., et al. 2006, *ApJ*, 640, 241
 Borch, A., Meisenheimer, K., Bell, E. F., et al. 2006, *A&A*, 453, 869
 Bottini, D., Garilli, B., Maccagni, D., et al. 2005, *PASP*, 117, 996
 Bower, R. G., Benson, A. J., Malbon, R., et al. 2006, *MNRAS*, 370, 645
 Brinchmann, J. & Ellis, R. S. 2000, *ApJ*, 536, L77
 Brown, M. J. I., Dey, A., Jannuzi, B. T., et al. 2007, *ApJ*, 654, 858
 Bruzual, G. 1983, *ApJ*, 273, 105
 Bruzual, G. & Charlot, S. 2003, *MNRAS*, 344, 1000
 Bundy, K., Ellis, R. S., & Conselice, C. J. 2005, *ApJ*, 625, 621
 Bundy, K., Ellis, R. S., Conselice, C. J., et al. 2006, *ApJ*, 651, 120
 Bundy, K., Treu, T., & Ellis, R. S. 2007, *ArXiv e-prints*, 705
 Cimatti, A., Daddi, E., Mignoli, M., et al. 2002, *A&A*, 381, L68
 Cimatti, A., Daddi, E., & Renzini, A. 2006, *A&A*, 453, L29
 Cimatti, A., Daddi, E., Renzini, A., et al. 2004, *Nature*, 430, 184
 Cowie, L. L., Songaila, A., Hu, E. M., & Cohen, J. G. 1996, *AJ*, 112, 839
 De Lucia, G., Springel, V., White, S. D. M., Croton, D., & Kauffmann, G. 2006, *MNRAS*, 366, 499
 Felten, J. E. 1976, *ApJ*, 207, 700
 Feulner, G., Gabasch, A., Salvato, M., et al. 2005a, *ApJ*, 633, L9
 Feulner, G., Goranova, Y., Drory, N., Hopp, U., & Bender, R. 2005b, *MNRAS*, 358, L1
 Fioc, M. & Rocca-Volmerange, B. 1997, *A&A*, 326, 950
 Fontana, A., Pozzetti, L., Donnarumma, I., et al. 2004, *A&A*, 424, 23
 Förster Schreiber, N. M., Genzel, R., Lehnert, M. D., et al. 2006, *ApJ*, 645, 1062
 Franzetti, P. 2005, Ph.D. Thesis, University of Milano Bicocca
 Franzetti, P., Scoddeggio, M., Garilli, B., et al. 2007, *A&A*, 465, 711
 Gallazzi, A., Charlot, S., Brinchmann, J., White, S. D. M., & Tremonti, C. A. 2005, *MNRAS*, 362, 41
 Gavazzi, G., Bonfanti, C., Sanvito, G., Boselli, A., & Scoddeggio, M. 2002, *ApJ*, 576, 135
 Genzel, R., Tacconi, L. J., Eisenhauer, F., et al. 2006, *Nature*, 442, 786
 Gialalisco, M., Ferguson, H. C., Koekemoer, A. M., et al. 2004, *ApJ*, 600, L93
 Guzman, R., Gallego, J., Koo, D. C., et al. 1997, *ApJ*, 489, 559
 Hamilton, D. 1985, *ApJ*, 297, 371
 Heavens, A., Panter, B., Jimenez, R., & Dunlop, J. 2004, *Nature*, 428, 625
 Hopkins, A. M. & Beacom, J. F. 2006, *ApJ*, 651, 142
 Ilbert, O., Tresse, L., Zucca, E., et al. 2005, *A&A*, 439, 863
 Iovino, A., McCracken, H. J., Garilli, B., et al. 2005, *A&A*, 442, 423
 Jimenez, R., Panter, B., Heavens, A. F., & Verde, L. 2005, *MNRAS*, 356, 495
 Juneau, S., Glazebrook, K., Crampton, D., et al. 2005, *ApJ*, 619, L135
 Kauffmann, G., Heckman, T. M., De Lucia, G., et al. 2006, *MNRAS*, 367, 1394
 Kauffmann, G., Heckman, T. M., White, S. D. M., et al. 2003a, *MNRAS*, 341, 33
 Kauffmann, G., Heckman, T. M., White, S. D. M., et al. 2003b, *MNRAS*, 341, 54
 Kennicutt, R. C. 1989, *ApJ*, 344, 685
 Kodama, T., Yamada, T., Akiyama, M., et al. 2004, *MNRAS*, 350, 1005
 Kriek, M., van Dokkum, P. G., Franx, M., et al. 2006, *ApJ*, 645, 44
 Labbé, I., Rudnick, G., Franx, M., et al. 2003, *ApJ*, 591, L95
 Lamareille, F., Contini, T., Brinchmann, J., et al. 2006, *A&A*, 448, 907
 Le Borgne, D., Abraham, R., Daniel, K., et al. 2006, *ApJ*, 642, 48
 Le Fèvre, O., Mellier, Y., McCracken, H. J., et al. 2004a, *A&A*, 417, 839
 Le Fèvre, O., Vettolani, G., Garilli, B., et al. 2005, *A&A*, 439, 845
 Le Fèvre, O., Vettolani, G., Paltani, S., et al. 2004b, *A&A*, 428, 1043

- Lilly, S. J., Le Fevre, O., Hammer, F., & Crampton, D. 1996, *ApJ*, 460, L1+
- Madau, P., Ferguson, H. C., Dickinson, M. E., et al. 1996, *MNRAS*, 283, 1388
- Martin, D. C., Wyder, T. K., Schiminovich, D., et al. 2007, *ArXiv Astrophysics e-prints*
- McCarthy, P. J., Le Borgne, D., Crampton, D., et al. 2004, *ApJ*, 614, L9
- McCracken, H. J., Radovich, M., Bertin, E., et al. 2003, *A&A*, 410, 17
- Mignoli, M., Cimatti, A., Zamorani, G., et al. 2005, *A&A*, 437, 883
- Miller, N. A. & Owen, F. N. 2002, *AJ*, 124, 2453
- Mouhcine, M., Lewis, I., Jones, B., et al. 2005, *MNRAS*, 362, 1143
- Neistein, E., van den Bosch, F. C., & Dekel, A. 2006, *MNRAS*, 372, 933
- Noeske, K. G., Faber, S. M., Weiner, B. J., et al. 2007, *ArXiv Astrophysics e-prints*
- Radovich, M., Arnaboldi, M., Ripepi, V., et al. 2004, *A&A*, 417, 51
- Renzini, A. 2006, *ARA&A*, 44, 141
- Renzini, A. 2007, *ArXiv Astrophysics e-prints*
- Salpeter, E. E. 1955, *ApJ*, 121, 161
- Savaglio, S., Glazebrook, K., Le Borgne, D., et al. 2005, *ApJ*, 635, 260
- Schmidt, M. 1968, *ApJ*, 151, 393
- Scodreggio, M., Franzetti, P., Garilli, B., et al. 2005, *PASP*, 117, 1284
- Stockton, A., Canalizo, G., & Maihara, T. 2004, *ApJ*, 605, 37
- Strateva, I., Ivezić, Ž., Knapp, G. R., et al. 2001, *AJ*, 122, 1861
- Thomas, D., Maraston, C., Bender, R., & Mendes de Oliveira, C. 2005, *ApJ*, 621, 673
- Tran, K.-V. H., van Dokkum, P., Franx, M., et al. 2005, *ApJ*, 627, L25
- Tremonti, C. A., Heckman, T. M., Kauffmann, G., et al. 2004, *ApJ*, 613, 898
- Tresse, L., Ilbert, O., Zucca, E., et al. 2006, *ArXiv Astrophysics e-prints*
- Tresse, L., Maddox, S., Loveday, J., & Singleton, C. 1999, *MNRAS*, 310, 262
- Zanichelli, A., Garilli, B., Scodreggio, M., et al. 2005, *PASP*, 117, 1271
- Zucca, E., Ilbert, O., Bardelli, S., et al. 2006, *A&A*, 455, 879

¹ IASF-INAF - via Bassini 15, I-20133, Milano, Italy e-mail: daniela@lambdate.inaf.it

² INAF-Osservatorio Astronomico di Brera - Via Brera 28, Milan, Italy

³ INAF-Osservatorio Astronomico di Bologna - Via Ranzani,1, I-40127, Bologna, Italy

⁴ Laboratoire d'Astrophysique de Marseille, UMR 6110 CNRS-Université de Provence, BP8, 13376 Marseille Cedex 12, France

⁵ Max Planck Institut für Astrophysik, 85741, Garching, Germany

⁶ Institut d'Astrophysique de Paris, UMR 7095, 98 bis Bvd Arago, 75014 Paris, France

⁷ Laboratoire d'Astrophysique de Toulouse/Tabres (UMR5572), CNRS, Université Paul Sabatier - Toulouse III, Observatoire Midi-Pyrénées, 14 av. E. Belin, F-31400 Toulouse (France)

⁸ IRA-INAF - Via Gobetti,101, I-40129, Bologna, Italy

⁹ INAF-Osservatorio Astronomico di Roma - Via di Frascati 33, I-00040, Monte Porzio Catone, Italy

¹⁰ School of Physics & Astronomy, University of Nottingham, University Park, Nottingham, NG72RD, UK

¹¹ Astrophysical Institute Potsdam, An der Sternwarte 16, D-14482 Potsdam, Germany

¹² Institute for Astronomy, 2680 Woodlawn Dr., University of Hawaii, Honolulu, Hawaii, 96822

¹³ Observatoire de Paris, LERMA, 61 Avenue de l'Observatoire, 75014 Paris, France

¹⁴ Università di Bologna, Dipartimento di Astronomia - Via Ranzani,1, I-40127, Bologna, Italy

¹⁵ Centre de Physique Théorique, UMR 6207 CNRS-Université de Provence, F-13288 Marseille France

¹⁶ Integral Science Data Centre, ch. d'Écogia 16, CH-1290 Versoix

¹⁷ Geneva Observatory, ch. des Maillettes 51, CH-1290 Sauverny, Switzerland

¹⁸ Astronomical Observatory of the Jagiellonian University, ul Orła 171, 30-244 Kraków, Poland

¹⁹ INAF-Osservatorio Astronomico di Capodimonte - Via Moiarriello 16, I-80131, Napoli, Italy

²⁰ Centro de Astrofísica da Universidade do Porto, Rua das Estrelas, 4150-762 Porto, Portugal

²¹ Università di Milano-Bicocca, Dipartimento di Fisica - Piazza delle Scienze, 3, I-20126 Milano, Italy